# Long-range interaction in waveguide lattices

Alexander Szameit,* Thomas Pertsch, Stefan Nolte, and Andreas Tünnermann†
*Institute of Applied Physics, Friedrich-Schiller-University Jena, Max-Wien-Platz 1, 07743 Jena, Germany*

Falk Lederer
*Institute for Condensed Matter Theory and Optics, Friedrich-Schiller-University Jena, Max-Wien-Platz 1, 07743 Jena, Germany*
(Received 8 January 2008; published 2 April 2008)

We introduce an analytical expression for the dynamics of light propagation in a two-dimensional waveguide lattice including general long range coupling. Additionally, the diffraction properties in such general systems are investigated in detail. Using these very general results, particular geometries are discussed, including the possibility of diffraction-free propagation in the center of the Brillouin zone. Furthermore, the transition from the discrete to the continuum limit is analyzed.

DOI: 10.1103/PhysRevA.77.043804 PACS number(s): 42.79.Gn, 42.82.Et, 42.25.Bs

## I. INTRODUCTION

Discreteness is a fundamental phenomenon which can be found in many aspects of modern physics such as quantum mechanics and solid state physics. However, most of the theoretical predictions concerning discrete systems are only hard to verify experimentally. Hence systems are required which exhibit similar structures in their physical behavior and mathematical formalism. Prominent examples for this type of system are arrays of evanescently coupled waveguides, which feature an inherent breaking of the isotropy of space. In waveguide arrays the transverse directions are physically different from the longitudinal direction of propagation, which is caused by the discreteness of the transverse coordinates. This is in strong contrast to homogeneous media. Hence discrete media exhibit a variety of new unusual effects such as unique imaging [1] and propagation [2] properties. Consequently, arrays of evanescently coupled waveguides present a wide field of research, which has been under investigation for decades. A great deal of theoretical and experimental work on discrete optical systems was initiated when discrete spatial solitary waves were predicted in waveguide arrays [3]. The experimental verification was performed in etched waveguides on a $Al_xGa_{1-x}As$ substrate [4], in optically induced waveguide arrays in photorefractive crystals [5], as well as in fs laser written waveguides [6]. Recently versatile technologies of fabricating even two-dimensional (2D) waveguide arrays were developed in photorefractive media [7,8] as well as in fs laser written waveguide arrays [9]. The key to understand nonlinear discrete propagation in 2D lattices is the analysis of the interaction of evanescent coupling between equivalent waveguides and nonlinear localization. In particular, this allows the investigation of 2D discrete spatial solitons [8,10,11] and surface lattice solitons [12,13], which are of high scientific interest since 2D spatial Kerr solitons are unstable in conventional isotropic media.

However, during the last years also a variety of interesting linear effects in waveguide arrays have been discovered and studied. Diffraction-free propagation [14,15], polychromatic diffraction in hexagonal [16,17] and one-dimensional (1D) curved lattices [18] was analyzed in detail as well as Zener tunneling [19], harmonic oscillation [20], the discrete Talbot effect [21] and quasi-incoherent propagation [22] in waveguide arrays. Furthermore, optical Bloch oscillations were theoretically predicted [23,24] and experimentally verified in 1D [25,26] and 2D [27] lattices.

The propagation of light in a lossless weakly coupled array of identical evenly spaced 2D homogeneous waveguides is usually modeled by a coupled mode approach. In this approximation only the amplitudes $\varphi_{m,n}(z)$ in the $m$th and $n$th waveguide in the horizontal and vertical directions, respectively, evolve during propagation while the field shapes remain constant. The transverse dynamics of the propagating field is induced by evanescent coupling of the waveguides, where energy exchange is caused by the overlap of the evanescent tails of the guided modes. In a conventional approximation, it is assumed that only neighboring waveguides interact and that higher-order interaction (i.e., interaction of nonadjacent guides) can be neglected. Then, the propagation of light in a 2D waveguide array can be adequately modeled by a set of coupled differential equations [28].

$$i\frac{d}{dz}\varphi_{m,n} + a(\varphi_{m+1,n} + \varphi_{m-1,n}) + b(\varphi_{m,n+1} + \varphi_{m,n-1}) + c(\varphi_{m+1,n+1} + \varphi_{m-1,n-1}) + d(\varphi_{m+1,n-1} + \varphi_{m-1,n+1}) = 0, \tag{1}$$

with the fast oscillating phase removed, $z$ as the propagation length, and where $a$, $b$, $c$, and $d$ are the coupling constants in horizontal, vertical, and diagonal directions, respectively, describing the strength of the evanescent coupling. This expression includes the particular cases of light propagation in a planar ($b=c=d=0$), square ($c=d=0$), and hexagonal ($d=0$) lattice. Recently, an analytical solution of this system was found for infinite and finite lattices [29]. However, assuming only next-neighbor waveguide interaction is a rather inaccurate approximation in the particular cases of long arrays or

*szameit@iap.uni-jena.de
†Also at Fraunhofer Institute for Applied Optics and Precision Engineering, Albert-Einstein-Strasse 7, 07745 Jena, Germany.

 

small waveguide separations. While the first case is intuitive, the latter can be demonstrated by a brief estimation. Since the coupling depends exponentially on the waveguide spacing $\Delta$ [30], the first-order coupling reads $\xi_1 = e^{-\Delta}$, while the second-order coupling is $\xi_2 = e^{-2\Delta}$. Hence the corresponding ratio of both coupling coefficients is $\xi_2/\xi_1 = e^{-\Delta}$. When the spacing is reduced to 50%, the according values read $\xi_1 = e^{-\Delta/2}$ and $\xi_2 = e^{-\Delta}$. Accordingly, the ratio increases to $\xi_2/\xi_1 = e^{-\Delta/2}$. Therefore the influence of higher-order coupling strongly depends on the separation of the individual waveguides. Following this argument, in the modeling of the light evolution the coupling of nonadjacent waveguides has to be taken into account. However, until now no analytical solution has been presented for either a 1D or a 2D discrete system, taking into account arbitrary orders of coupling between the single lattice sites.

In this paper we introduce an analytic expression to describe the evolution of the amplitudes in a infinite 2D waveguide array with arbitrary coupling of all waveguides in all directions, representing the Green's function of the system. Furthermore, the light diffraction in such general systems is analyzed in detail, revealing modified conditions for diffraction-free propagation compared to conventional systems with only next-neighbor interaction. In addition, the continuum limit of the discrete propagation equations is derived, pointing out the strong correspondence between evanescent coupling in discrete media and diffraction in continuous media.

## II. ANALYTICAL SOLUTION

To describe the coupling in an arbitrary waveguide array, the coupled mode equations (1) are extended to cover general higher-order coupling. This results in the generalized coupled mode equations

$$i\frac{d}{dz}\varphi_{m,n} + \sum_{\alpha=-\mu}^{\mu}\sum_{\beta=-\nu}^{\nu}\xi_{\alpha,\beta}\varphi_{m+\alpha,n+\beta} = 0 \tag{2}$$

with $\varphi_{m,n}$ as the amplitude in the $m$, $n$th waveguide. The coupling constants $\xi_{\alpha,\beta}$ between the single guides are shown in Fig. 1. For symmetry reasons one finds $\xi_{\alpha,\beta} = \xi_{-\alpha,-\beta}$. The values $\mu, \nu$ represent the maximum order of coupling in the $m$ and $n$ directions, respectively. When only next-neighbor interaction is assumed in $m$ direction it is $\mu = 1$, for second-order interaction, $\mu = 2$, and so on. Theoretically, $\mu$ and $\nu$ can be set to infinity.

The value $\xi_{0,0}$ can be interpreted as self-coupling within the waveguides and is set to zero since self-coupling can be normalized by a simple coordinate transformation. The coupling constants of Eq. (1) are represented in Eq. (2) by $\xi_{1,0} = a$, $\xi_{0,1} = b$, $\xi_{1,1} = c$, and $\xi_{1,-1} = d$. Using

$$\varphi_{m,n}(z) = \int_{-\pi}^{\pi}\int_{-\pi}^{\pi} d\kappa_m d\kappa_n \tilde{\varphi}(\kappa_m, \kappa_n, z)\exp\{-i(\kappa_m m + \kappa_n n)\},$$

$$\tilde{\varphi}(\kappa_m, \kappa_n, z) = \frac{1}{(2\pi)^2}\sum_{m,n}\varphi_{m,n}(z)\exp\{i(\kappa_m m + \kappa_n n)\} \tag{3}$$

as the corresponding Fourier pair of amplitudes and $\kappa_m$ and $\kappa_n$ as the wave numbers in the horizontal and vertical directions, respectively, one can perform a discrete transform of Eq. (2) into the Fourier space. This yields

$$\left(i\frac{\partial}{\partial z} + \sum_{\alpha=-\mu}^{\mu}\sum_{\beta=-\nu}^{\nu}\xi_{\alpha,\beta}e^{i\alpha\kappa_m}e^{i\beta\kappa_n}\right)\tilde{\varphi}(\kappa_m, \kappa_n, z) = 0. \tag{4}$$

The solution of Eq. (4) is

$$\tilde{\varphi}(\kappa_m, \kappa_n, z) = \prod_{\alpha=1}^{\mu}\prod_{\beta=1}^{\nu} e^{2iz\xi_{\alpha,0}\cos\{\alpha\kappa_m\}}e^{2iz\xi_{0,\beta}\cos\{\beta\kappa_n\}} \times e^{2iz\xi_{\alpha,\beta}\cos\{\alpha\kappa_m+\beta\kappa_n\}}e^{2iz\xi_{\alpha,-\beta}\cos\{\alpha\kappa_m-\beta\kappa_n\}}. \tag{5}$$

After an inverse Fourier transformation, using the identity (for more information please see also Ref. [29])

$$\sum_k i^k J_k(x)e^{i\beta k} = e^{ix\cos\beta}, \tag{6}$$

one obtains the solution of Eq. (2),

$$\varphi_{m,n}(z) = i^{m+n}\sum J_{m-\sum_{\gamma=2}^{\mu}\gamma k_\gamma - \sum_{\alpha=1}^{\mu}\sum_{\beta=1}^{\nu}\alpha(s_\alpha^\beta + t_\alpha^\beta)}(2z\xi_{1,0})J_{n-\sum_{\delta=2}^{\nu}\delta r_\delta - \sum_{\beta=1}^{\nu}\sum_{\alpha=1}^{\mu}\beta(s_\alpha^\beta - t_\alpha^\beta)}(2z\xi_{0,1})\left(\prod_{\gamma=2}^{\mu} i^{[\gamma-1]k_\gamma}J_{k_\gamma}(2z\xi_{\gamma,0})\right) \times\left(\prod_{\delta=2}^{\nu} i^{-([\delta-1]\,r_\delta}J_{r_\delta}(2z\xi_{0,\delta})\right)\left(\prod_{\alpha=1}^{\mu}\prod_{\beta=1}^{\nu} i^{-([\alpha+\beta-1]s_\alpha^\beta + [\alpha-\beta-1]t_\alpha^\beta)}J_{s_\alpha^\beta}(2z\xi_{\alpha,\beta})J_{t_\alpha^\beta}(2z\xi_{\alpha,-\beta})\right). \tag{7}$$

Here, $J_n(x)$ are Bessel functions of the first kind of order $n$. The sum in Eq. (7) denotes the summation over all values $k_2, \ldots, k_\mu, r_2, \ldots, r_\nu, s_1^1, \ldots, s_\mu^\nu, t_1^1, \ldots, t_\mu^\nu$. The first line of Eq. (7) represents to some extent the superposition of the amplitudes in a horizontal and vertical 1D waveguide array. These expressions are coupled by the terms in the second and third line. The expression in the second line is caused by the influence of the long-range interaction, while the terms in the third line describe the diagonal coupling.

## III. LIMITING CASES

The very general expression (7) describes the light evolution in a general lattice where all waveguides interact. How-

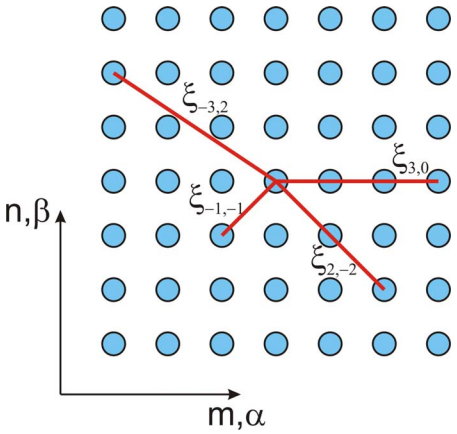


FIG. 1. (Color online) Some examples of coupling constants $\xi_{\alpha,\beta}$.

ever, for particular cases this formula can be simplified.

### A. General 2D lattice with only first-order coupling

One important setup is the general 2D lattice with only first-order coupling ($\mu=\nu=1$). Hence one finds that $\gamma=\delta=0$ yielding directly $\xi_{\gamma,0}=\xi_{0,\delta}=k_\gamma=r_\delta=0$ and $\alpha=\beta=1$. This results in the expression

$$\varphi_{m,n}(z) = i^{m+n} \sum_{s_1^1,t_1^1} i^{-s_1^1+t_1^1} J_{m-s_1^1-t_1^1}(2z\xi_{1,0}) J_{n-s_1^1+t_1^1}(2z\xi_{0,1}) \times J_{s_1^1}(2z\xi_{1,1}) J_{t_1^1}(2z\xi_{1,-1}), \tag{8}$$

which is identical to the corresponding expression in Ref. [29]. In physical terms this equation represents the superposition of amplitudes caused by virtual sources at positions $s_1^1+t_1^1$, $s_1^1-t_1^1$ weighted by multiplicative factors $J_{s_1^1}(2z\xi_{1,1})J_{t_1^1}(2z\xi_{1,1})$.

### B. 1D lattice with higher-order coupling

Another important limiting case is the 1D waveguide array with higher-order waveguide interaction [Fig. 2(a)]. Here it is $\xi_{\alpha,\beta}=0 \ \forall \beta\neq 0$ and $\nu=0$ and hence $\xi_{0,\delta}=r_\delta=s_\alpha^\beta=t_\alpha^\beta=0$. With this, one arrives at

$$\varphi_m(z) = i^m \sum_{k_2,\ldots,k_\mu} J_{m-\sum_{\gamma=2}^{\mu}\gamma k_\gamma}(2z\xi_1) \prod_{\gamma=2}^{\mu} i^{-[\gamma-1]k_\gamma} J_{k_\gamma}(2z\xi_\gamma) \tag{9}$$

where the abbreviated notation $\xi_1=\xi_{1,0}$ and $\xi_\gamma=\xi_{\gamma,0}$ was used. As a convention, the propagation distance will be given in terms of coupling lengths $l_c=\pi/2\xi_1$. The infinite sum can be truncated according to Ref. [29]. For large orders $m$ for the first maximum $x_m$ of a Bessel function $J_m(x_m)$ the relation

$$x_m \approx m \tag{10}$$

holds. It is assumed that a contributing Bessel function has to reach at least its first maximum to give a significant contribution. Hence every sum can be truncated approximately at

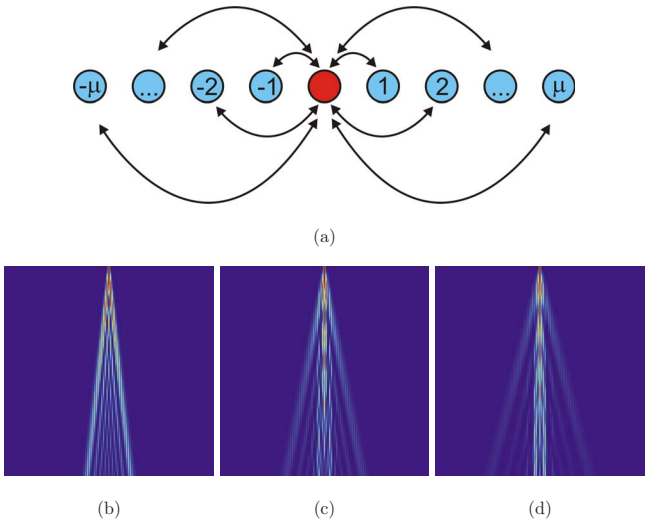


FIG. 2. (Color online) (a) Higher-order waveguide interaction in a 1D lattice. When a single waveguide is excited, the light couples to all neighboring guides with the coupling constants $\xi_1,\xi_2,\ldots,\xi_\mu$. In (b) the propagation pattern of a waveguide array after $4.5l_c$ is shown, when only next-neighbor interaction $\xi_1=1$ is taken into account. When additionally second-order coupling is taken into account with $\xi_2=0.5$, the resulting output pattern changes (c). A further consideration of third-order coupling $\xi_3=0.25$ yields the pattern shown in (d). A particular feature is the stronger broadening of the side lobes of the light patterns and a stronger localization around the excited waveguide with increasing higher-order coupling from (b) to (d). In all figures, the propagation direction is from top to bottom, while the waveguide numbering goes from left to right.

$$k_{\gamma,\max} \approx 2z\xi_\gamma. \tag{11}$$

Inserting this into the indices of the first Bessel function in Eq. (9), one arrives at the relation

$$m_{\max} - \sum_{\gamma=2}^{\mu} \gamma 2z\xi_\gamma = 2z\xi_1. \tag{12}$$

Hence the approximate width of a propagating light pattern is given as

$$m_{\max} = 2z\left(\sum_{\gamma=1}^{\mu} \gamma\xi_\gamma\right). \tag{13}$$

The width $m_{\max}$ is a crucial attribute for propagating light which experiences higher-order coupling. According to Eq. (13) this results in a stronger broadening of the propagating field. However, it turns out that the propagation pattern in the array does not only broaden but changes significantly for an increasing influence of higher-order coupling. As an example, in Fig. 2(b) the propagation with only next-neighbor interaction after a propagation distance of $4.5l_c$ is shown, where $\xi_1=1$. In Fig. 2(c) the second-order interaction is set to $\xi_2=0.5$, while the propagation distance is kept. The influence of an additional third-order coupling with $\xi_3=0.25$ is demonstrated in Fig. 2(d). An intriguing feature of the according propagation pattern is that, besides a stronger divergence of the side lobes, the main fraction of the propagating

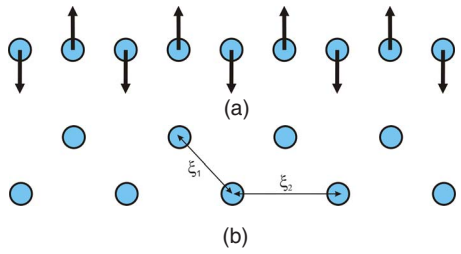


FIG. 3. (Color online) (a) Implementation of a zigzag configuration of waveguides for the experimental investigation of second-order coupling. (b) First-order $\xi_1$ and second-order coupling $\xi_2$ in a zigzag array.

light remains more and more localized around the excited waveguide for increasing higher-order coupling. This interesting behavior is caused by a modification of the band structure and will be discussed in detail in the next section.

However, in planar setups the evanescent coupling usually decreases exponentially, which makes it difficult to tune the range of the coupling. To overcome this, a sophisticated implementation is the extension of a 1D lattice into the second transverse dimension [see Fig. 3(a)]. The waveguides are alternately shifted up and down to achieve a zigzag arrangement [31], which is the basis for the experimental tuning of second-order coupling by precisely adjusting the transverse shift of the waveguides [Fig. 3(b)]. The fabrication of such a device can be achieved in particular using the fs laser writing technique, with which large two-dimensional lattices with arbitrary topology can be fabricated [16,30]. In the zigzag array the two coupling constants $\xi_1$ and $\xi_2$ can be individually tuned by the waveguide separation. This provides the feasibility for the detailed analysis of a variety of arrangements for the ratio $\xi_2/\xi_1$. A case of particular interest is when $\xi_2/\xi_1 > 1$, where the unique situation is met that the second-order coupling is stronger than the first-order coupling.

In such a geometry, one finds mainly first and second order coupling, so that the light evolution is described by the equation

$$\varphi_m(z) = \sum_k i^{m-k} J_{m-2k}(2zc_1) J_k(2zc_2), \tag{14}$$

which can be derived from Eq. (7) using $k=k_2$, $c_1=\xi_{1,0}$, and $c_2=\xi_{2,0}$. An increasing ratio $c_2/c_1$ yields considerable variations of the light evolutions. In Fig. 4(b) the black dashed line shows the output pattern of a 1D lattice with only first-order coupling after a propagation distance of $13l_c$. When taking the second-order coupling into account with a strength of $\xi_2=0.1\xi_1$, then the corresponding output pattern changes, which is shown by the solid red line in Fig. 4(b). Due to Eq. (13) the field broadens stronger under the influence of the second-order coupling and, again, a significant fraction of the light remains close to the excited waveguide.

## IV. DIFFRACTION WITH LONG-RANGE INTERACTION

A convenient tool for the investigation of the propagation properties of the evolving light is the dispersion relation of a medium, which connects transverse and longitudinal phase

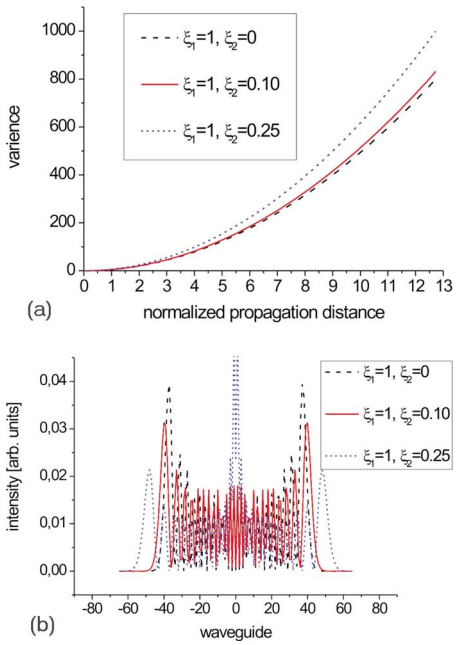


FIG. 4. (Color online) Comparison of the amplitude distribution in a planar array with only first order coupling (black dashed line) and additional second order coupling, when $\xi_2=0.1\xi_1$ (red solid line) and $\xi_2=0.25\xi_1$ (blue dotted line). In (a) the evolution of the variance of the light pattern is shown. The shape of the output patterns after a propagation length of $13l_c$ are shown in (b).

evolution for a fixed optical frequency. The eigenmodes of a general waveguide lattice with higher-order coupling are plane waves and read as

$$\varphi_{m,n} = \varphi_0 e^{i\kappa_m m} e^{i\kappa_n n} e^{i\kappa_z z} \tag{15}$$

with $\kappa_z$ as the longitudinal and $\kappa_m$, $\kappa_n$ as the normalized transverse wave numbers. Inserting Eq. (15) into Eq. (2), one obtains the general dispersion relation, which connects the longitudinal and the transverse wave numbers and reads as

$$\kappa_z = \frac{1}{2} \sum_{\alpha=-\mu}^{\mu} \sum_{\beta=-\nu}^{\nu} \xi_{\alpha,\beta} \cos\{\alpha\kappa_m + \beta\kappa_n\} + \xi_{\alpha,-\beta} \cos\{\alpha\kappa_m - \beta\kappa_n\}, \tag{16}$$

where the self-coupling is again assumed to be normalized, i.e., $\xi_{0,0}=0$. The transverse wave numbers $\kappa_m$, $\kappa_n$ represent the phase shift among successive lattice sites and play the role of a "particle momentum." They may be introduced by exciting several waveguides and tilting the beam [32]. In Fig. 5 different dispersion relations are shown. The case $\xi_{1\text{st order}}=1$, $\xi_{\text{order}>1}=0$ is shown in Fig. 5(a), the case $\xi_{1\text{st order}}=1$, $\xi_{2\text{nd order}}=0.5$, $\xi_{\text{order}>2}=0$ is illustrated in Fig. 5(b), and the dispersion relation for $\xi_{1\text{st order}}=1$, $\xi_{2\text{nd order}}=0.5$, $\xi_{3\text{rd order}}=0.25$, $\xi_{\text{order}>3}=0$ is shown in Fig. 5(c). For increasing higher-order coupling a growth of the maximal longitudinal wave number $\kappa_z$ is observed as well as a narrowing of the central maximum. This involves a flattening of the dispersion relation in the outer regions of the Brillouin zone, which is important for the analysis of the diffraction in lattices with higher-order coupling.

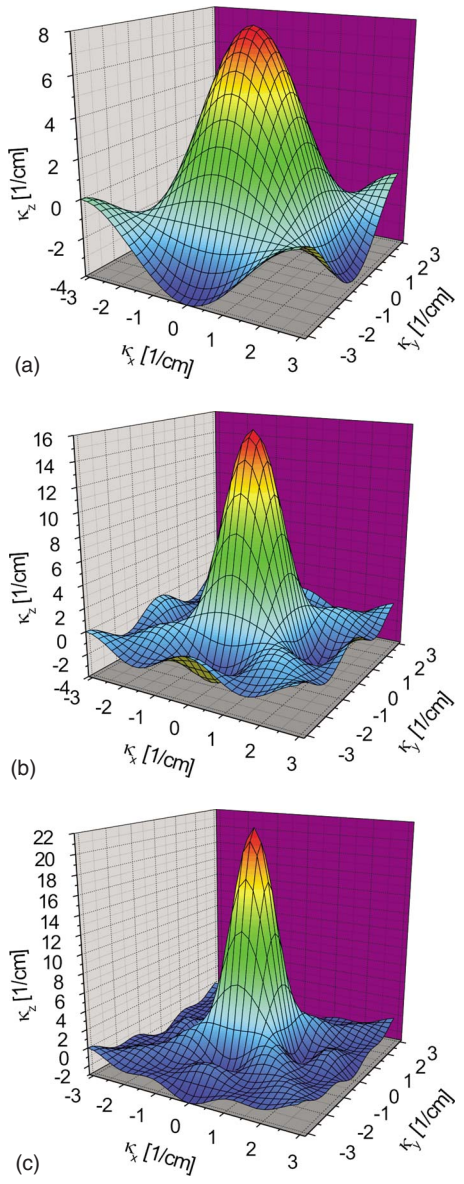


FIG. 5. (Color online) The dispersion relation for a lattice with symmetric first-order coupling $\xi_{1\text{st order}}$ is shown in (a), for a lattice with second-order coupling $\xi_{2\text{nd order}}=0.5\times\xi_{1\text{st order}}$ is shown in (b) and a dispersion relation for a lattice with $\xi_{3\text{rd order}}=0.5\times\xi_{2\text{nd order}}=0.25\times\xi_{1\text{st order}}$ is shown in (c). The center peak growths and narrows for increasing coupling order, while the outer regions of the dispersion relation flatten.

The diffraction strength of the propagating beam is given by the second derivative of Eq. (16) [2,29]

$$\frac{\partial^2\kappa_z}{\partial\kappa_m^2} = -\frac{1}{2}\sum_{\alpha=-\mu}^{\mu}\sum_{\beta=-\nu}^{\nu}\alpha^2(\xi_{\alpha,\beta}\cos\{\alpha\kappa_m+\beta\kappa_n\} + \xi_{\alpha,-\beta}\cos\{\alpha\kappa_m-\beta\kappa_n\}), \tag{17}$$

$$\frac{\partial^2\kappa_z}{\partial\kappa_n^2} = -\frac{1}{2}\sum_{\alpha=-\mu}^{\mu}\sum_{\beta=-\nu}^{\nu}\beta^2(\xi_{\alpha,\beta}\cos\{\alpha\kappa_m+\beta\kappa_n\} + \xi_{\alpha,-\beta}\cos\{\alpha\kappa_m-\beta\kappa_n\}). \tag{18}$$

### A. Diffraction-free propagation in 2D

Diffraction-free propagation is obtained when $\partial^2\kappa_z/\partial\kappa_m^2=\partial^2\kappa_z/\partial\kappa_n^2=0$. In the following, a symmetric lattice will be considered, where one finds $\xi_{\alpha,0}=\xi_{0,\beta}$ for $\alpha=\beta$ and $\xi_{\alpha,\beta}=\xi_{\alpha,-\beta}$ and $\xi_{\alpha,\beta}=\xi_{-\alpha,\beta}$ for arbitrary values of $\alpha$ and $\beta$. Hence in the diffraction-free case, subtracting Eq. (18) from Eq. (17) yields the condition

$$\sum_{\alpha=1}^{\mu}\alpha^2\xi_{\alpha,0}\cos\{\alpha\kappa_m\} = \sum_{\beta=1}^{\mu}\beta^2\xi_{0,\beta}\cos\{\beta\kappa_n\}. \tag{19}$$

Due to $\xi_{\alpha,0}=\xi_{0,\beta}$ for $\alpha=\beta$ this is equivalent to the condition

$$\sum_{\alpha=1}^{\mu}\alpha^2\xi_{\alpha,0}(\cos\{\alpha\kappa_m\}-\cos\{\alpha\kappa_n\}) = 0. \tag{20}$$

Within the first Brillouin zone ($-\pi\leq\kappa_m,\kappa_n\leq\pi$), a solution is $\kappa_m=\pm\kappa_n$. Inserting this into Eqs. (17) and (18) results in single isolated points in the first Brillouin zone, where the propagation is diffraction free. For $\mu=\nu=1$ this is the only solution [29]. However, for $(\mu=\nu)>1$ more solutions exist whose number is determined by the coupling coefficients and, in particular, by the order of the coupling. To solve Eq. (20) for both $\kappa_m$ and $\kappa_n$ it is required that

$$\sum_{\alpha=1}^{\mu}\alpha^2\xi_{\alpha}\cos\{\alpha\kappa_j\} = \eta(\kappa_j), \tag{21}$$

where $\kappa_j=\kappa_m=\kappa_n$ and $\eta(\kappa_m)=\eta(\kappa_n)$. For $\mu>1$, the function $f(x)=\Sigma_{\alpha=1}^{\mu}\alpha^2\xi_{\alpha}\cos\{\alpha x\}$ exhibits local extrema, in whose vicinity two different values of $\kappa_j$ fulfill the condition (21) for a given value $\eta(\kappa_j)$. In the general case, the number of local extrema gives an upper limit for the number of possible combinations $(\kappa_m;\kappa_n)$ yielding the same $\eta(\kappa_j)$. This is shown in Fig. 6(a), where $\eta(\kappa_j)=-0.75$, $\mu=\nu=3$ and $\xi_{1,0}=1$, $\xi_{2,0}=0.3$, and $\xi_{3,0}=0.2$.

To estimate the number of possible combinations $(\kappa_m;\kappa_n)$, one has to take the extreme values of the function $\eta(\kappa_j)$ into account, which are defined by

$$\frac{\partial\eta(\kappa_j)}{\partial\kappa_j} = -\sum_{\alpha=1}^{\mu}\alpha^3\xi_{\alpha}\sin\{\alpha\kappa_j\}\stackrel{!}{=}0. \tag{22}$$

Due to the polynomial character of the equation, within the first Brillouin zone, there are $\mu+1$ roots, each corresponding to a maximum of Eq. (21). Furthermore, obviously three roots of this equation can be always found in the center and at the edge of the first Brillouin zone ($\kappa_j=0,\pm\pi$). Hence Eq. (21) exhibits $2\mu+1$ extreme values and, therefore, $2\mu$ combinations $(\kappa_m;\pm\kappa_{n_1},\pm\kappa_{n_2},\pm\kappa_{n_\mu})$ exist for every value of $\eta(\kappa_j)$. This results in a variety of directions, in which diffraction-free propagation is possible. They occur not only as single points in the first Brillouin zone [Fig. 6(b)], but as extended contours as shown in Fig. 6(c), which is solely caused by the higher-order coupling.

### B. Diffraction-free propagation in 1D

Further peculiarities of propagation in lattices exhibiting higher-order coupling become evident in particular in 1D lattices. The 1D dispersion relation reads as

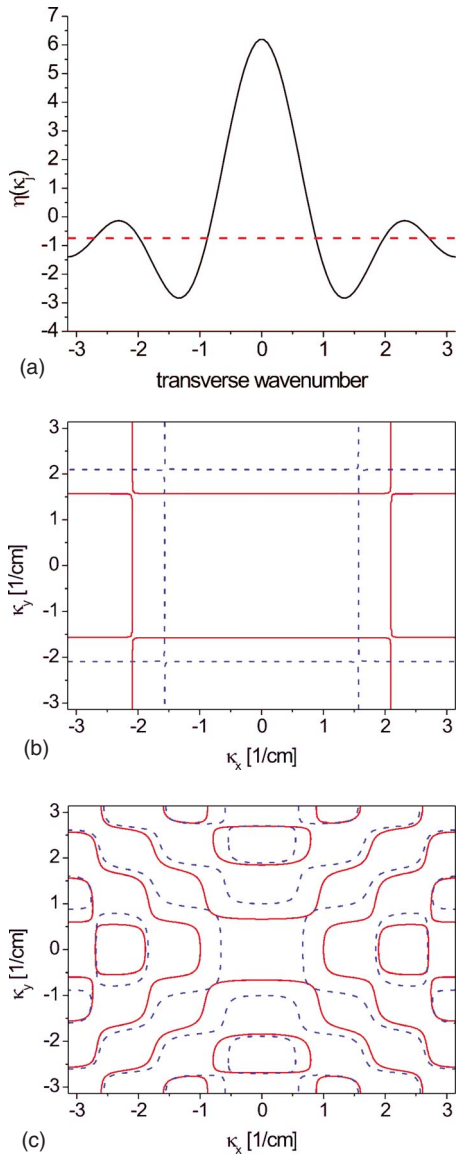


FIG. 6. (Color online) (a) The function Eq. (21) within the first Brillouin zone. The intersections with the dashed line mark six values of $\kappa_j$ which yield $\eta(\kappa_j)=-0.75$. (b) Zeros of Eq. (17) (red, solid) and Eq. (18) (blue, dashed) indicating diffraction-free propagation in the $m$ and $n$ direction in a lattice with only first-order symmetric coupling $\xi_{1,0}=\xi_{0,1}=\xi_{1,1}=\xi_{1,-1}$. The intersection of both lines yields the values of the corresponding transverse wave numbers for total diffraction-free propagation. In a lattice with only first-order coupling these are single points. (c) In contrast for a lattice with coupling up to the third order ($\xi_{3\text{rd order}}=0.5\times\xi_{2\text{nd order}}=0.25\times\xi_{1\text{st order}}$) the intersection of the zeros can be extended regions, in which diffraction-free propagation is possible.

$$\kappa_z=\sum_{\alpha=1}^{\mu}2\xi_\alpha\cos\{\alpha\kappa_m\}, \tag{23}$$

and the corresponding condition for diffraction-free propagation is given as

$$\frac{\partial^2\kappa_z}{\partial\kappa_m^2}=-\sum_{\alpha=1}^{\mu}2\alpha^2\xi_\alpha\cos\{\alpha\kappa_m\}\stackrel{!}{=}0, \tag{24}$$

which is a special case of Eq. (21). Diffraction-free propagation with only next-neighbor interaction (i.e., $\mu=1$) is obtained for $\kappa_m=\pi/2$ since

$$\cos\{\kappa_m\}\stackrel{!}{=}0\Rightarrow\kappa_m=\frac{\pi}{2}. \tag{25}$$

However, including higher-order coupling reduces the angle for the diffraction-free propagation. An interesting result is obtained for the particular case of $\xi_1=4\xi_2$, which directly yields

$$\cos\{\kappa_m\}+\cos\{2\kappa_m\}\stackrel{!}{=}0\Rightarrow\kappa_m=\frac{\pi}{3} \tag{26}$$

and in general for $\mu$th-order coupling with $\xi_1=4\xi_2=\cdots=\mu^2\xi_\mu$, one obtains

$$\sum_{\alpha=1}^{\mu}\cos\{\alpha\kappa_m\}\stackrel{!}{=}0\Rightarrow\kappa_m=\frac{\pi}{\mu+1}. \tag{27}$$

Hence for sufficiently strong higher-order coupling, the angle for diffraction-free propagation is significantly reduced.

A completely new situation can be obtained when negative coupling constants are introduced. In the case of second order-coupling the condition for diffraction-free propagation according to Eq. (24) is

$$\xi_1\cos\{\kappa_m\}=-4\xi_2\cos\{2\kappa_m\}. \tag{28}$$

If one chooses $\xi_1=-4\xi_2$, diffraction-free propagation is obtained for $\kappa_m=0$, which is in the center of the first Brillouin zone. In addition, this interesting behavior can be achieved for every even $\mu$, where, e.g., $\xi_1=-4\xi_2=9\xi_3=\cdots=-\mu^2\xi_\mu$. Negative coupling constants are physically equivalent to an additional phase shift of $\pi$ caused by the coupling. However, this is not feasible for pure evanescent coupling which induces no additional phase shift. Hence this effect is not observable in conventional waveguide lattices. For a possible experimental realization one has to use a different coupling mechanism, which is found, e.g., in radiative coupling, as it occurs in so-called Bragg waveguides [33]. A particular implementation of such waveguides are defects in photonic crystals [34,35]. Due to the periodicity of this medium the wave number of the light lies within a band gap, so that the light propagation inside the medium is forbidden. Hence light is confined in artificial defects which then act as waveguides. The waveguide modes, also called leaky modes, steadily emit radiation, which in turn can excite modes in adjacent defect waveguides. With such a Bragg waveguide lattice, the coupling can be tuned appropriately to meet the conditions given above for diffraction-free propagation in the center of the Brillouin zone. Hence lattices of coupled Bragg waveguides provide an excellent base for the investigation of these new and interesting discrete propagation effects.

## V. CONTINUUM LIMIT

In the following, the transition from the discrete regime to the continuum limit will be analyzed. For reasons of simplicity the considerations are restricted to a 1D lattice but can be easily extended to the 2D case. For well-separated waveguides, higher-order coupling can be neglected and the coupled mode equations [Eq. (2)] simplify to

$$i\frac{d}{dz}\varphi_m(z) + \xi_1[\varphi_{m+1}(z) + \varphi_{m-1}(z)] = 0 \tag{29}$$

with $\xi_1$ as the first-order coupling constant. For a broad excitation covering multiple waveguides under normal incidence (so that no phase shift between adjacent guides is introduced), the amplitudes vary only slowly over a number of waveguides. Then, one can define a transversely extended function $q(x,z)$, which is connected to the modal amplitudes $\varphi_m(z)$ by

$$\varphi_m(z) = q(x,z)e^{2i\xi_1 z}, \tag{30}$$

where $\Delta$ is the waveguide spacing and $x=m\Delta$. Inserting this in Eq. (29) and using the discrete transverse second derivative

$$\varphi_m^{(2)} = \frac{\varphi_{m+1} + \varphi_{m-1} - 2\varphi_m}{\Delta^2} \tag{31}$$

yields

$$\left(i\frac{\partial}{\partial z} + \xi_1\Delta^2\frac{\partial^2}{\partial x^2}\right)q(x,z) = 0, \tag{32}$$

which is the paraxial Helmholtz equation, describing the beam evolution in a waveguide layer. Hence for broad normal incident excitation, the discrete character of the light evolution disappears and the intensity distribution inside the waveguides is equivalent to a single continuous layer. Accordingly, the dispersion relation can be obtained by substituting the plane wave solution $q(x,z)=\exp\{i(\kappa_x x+\kappa_z z)\}$ into Eq. (32) yielding the parabolic relation

$$\kappa_z = -\xi_1\Delta^2\kappa_x^2. \tag{33}$$

However, the question arises what happens if the waveguide separation is in a domain where higher-order coupling has to be taken into account. In this case the coupled mode equations [Eq. (2)] reduce only to

$$i\frac{d}{dz}\varphi_m(z) + \sum_{j=1}^{\mu}\xi_j[\varphi_{m+j}(z) + \varphi_{m-j}(z)] = 0, \tag{34}$$

while the higher-order coupling pendant of Eq. (30) reads as

$$\varphi_m(x) = q(x,z)\prod_{\rho=1}^{\mu} e^{2i\xi_\rho z}. \tag{35}$$

For the transformation into the continuum limit, one has to deal with higher-order discrete derivatives. The coefficients of the derivatives follow a modified Pascal's triangle [36], which is given as

$$\begin{array}{ccccccccccccc}
 & & & & & & 1 & & & & & & \\
 & & & & & 1 & & -1 & & & & & \\
 & & & & 1 & & -2 & & 1 & & & & \\
 & & & 1 & & -3 & & 3 & & -1 & & & \\
 & & 1 & & -4 & & 6 & & -4 & & 1 & & \\
 & 1 & & -5 & & 10 & & -10 & & 5 & & -1 & \\
1 & & -6 & & 15 & & -20 & & 15 & & -6 & & 1 \\
\iddots & & & & & & \vdots & & & & & & \ddots
\end{array}$$

Hence the discrete derivatives of even order read as (note that the argument has been omitted)

$$\varphi_m^{(2\mu)} = \frac{1}{\Delta^{2\mu}}\sum_{j=0}^{2\mu}(-1)^j\binom{2\mu}{j}\varphi_{m+\mu-j}. \tag{36}$$

Inserting Eq. (35) into Eq. (34), the continuum limit considering higher-order coupling up to the order $\mu$ is found to be

$$\left(i\frac{\partial}{\partial z} + \sum_{\rho=1}^{\mu}\xi_\rho\sum_{\sigma=0}^{\rho-1}A_\sigma^\rho\Delta^{2(\rho-\sigma)}\frac{\partial^{2(\rho-\sigma)}}{\partial x^{2(\rho-\sigma)}}\right)q(x,z) = 0 \tag{37}$$

with some coefficients $A_\sigma^\rho$ with $\rho \geq 1$, which are defined by $A_0^\rho=1$ and for $\sigma>0$ by the recurrence formula

$$A_\sigma^\rho = \sum_{j=1}^{\sigma}(-1)^{j-1}\binom{2(\rho-\sigma+j)}{j}A_{\sigma-j}^\rho. \tag{38}$$

A particular feature of Eq. (37) is the appearance of higher-order differentials. As a result, the dispersion relation in the continuum limit is no longer purely parabolic, but includes

higher orders of the transverse wave number:

$$\kappa_z = -\sum_{\rho=1}^{\mu} \xi_\rho \sum_{\sigma=0}^{\rho-1} A_\sigma^\rho \Delta^{2(\rho-\sigma)} \kappa_x^{2(\rho-\sigma)}. \tag{39}$$

Hence including higher-order coupling into the propagation equations (34) results in a deformation of the band structure of the propagation constants due to the modified dispersion relation Eq. (39). Thus, the continuum limit Eq. (32) of a waveguide layer is only valid for broad excitations when the single guides are sufficiently separated, i.e., the higher-order coupling is negligible. In contrast, for decreasing waveguide separations the higher-order coupling gives significant contributions, so that one arrives at Eq. (39). Hence within the coupled mode approximation an increase of the width of the excitation is physically not equivalent to a decrease of the waveguide separation at a constant excitation width.

However, for very broad excitations in Eq. (37) only the second-order derivatives give a significant contribution and the higher-order derivatives $\partial^4/\partial x^4, \ldots, \partial^{2\mu}/\partial x^{2\mu}$ can be neglected, since the amplitudes change only marginally between adjacent guides. Furthermore, one can show that the relation

$$A_{\rho-1}^\rho = \rho^2 \tag{40}$$

holds. Then, Eq. (37) simplifies to

$$\left( i\frac{\partial}{\partial z} + \Delta^2 \frac{\partial^2}{\partial x^2} \sum_{\rho=1}^{\mu} \xi_\rho \rho^2 \right) q(x,z) = 0. \tag{41}$$

One particular solution of the paraxial Helmholtz equation is a Gaussian beam. The term $\Sigma_{\rho=1}^{\mu} \xi_\rho \rho^2$ has a direct impact on the divergence of the beam inside the lattice in the continuum limit. Hence the coupling coefficients $\xi_\rho$ are the analog to the wavelength in the continuum limit. The higher-order coupling constants cause a strong broadening of the beam caused by the quadratic coefficients $\rho^2$. For instance, in the case that $\xi_{\rho>2}=0$ and $\xi_1 \approx \xi_2$ the divergence is five times larger than for pure first order coupling ($\xi_2=0$).

For a further investigation it is useful to reduce Eq. (41) once more by defining

$$\xi_2 = \alpha_1 \xi_1,$$

$$\xi_3 = \alpha_2 \xi_2 = \alpha_2 \alpha_1 \xi_1,$$

$$\vdots$$

$$\xi_\rho = \xi_1 \prod_{j=0}^{\rho} \alpha_j, \tag{42}$$

with $\alpha_0 := 1$, so that it takes the form

$$\left( i\frac{\partial}{\partial z} + \xi_1 \Delta^2 \frac{\partial^2}{\partial x^2} \sum_{\rho=1}^{\mu} \rho^2 \prod_{j=0}^{\rho-1} \alpha_j \right) q(x,z) = 0. \tag{43}$$

Now, the investigation of the broadening of the propagating beam reduces to the analysis of the series

$$\zeta(\mu) = \sum_{\rho=1}^{\mu} \rho^2 \prod_{j=0}^{\rho-1} \alpha_j. \tag{44}$$

The sum $\zeta(\mu)$ corresponds to a value which gives the relative broadening of the beam in comparison to first-order coupling as it is obtained in Eq. (32).

A particular situation is the exponential decay of the coupling constants. In this case, a decay constant $\delta$ is defined with $\alpha_1 = \cdots = \alpha_\rho = e^{-\delta}$, which is used in the relations

$$\xi_2 = e^{-\delta} \xi_1,$$

$$\xi_3 = e^{-\delta} \xi_2 = e^{-2\delta} \xi_1,$$

$$\vdots$$

$$\xi_\rho = \xi_1 e^{-(\rho-1)\delta}. \tag{45}$$

In addition, due to the exponential decay one can assume $\mu \to \infty$. Consequently, the diffraction is described by the infinite series

$$\tilde{\zeta}(\delta) = \sum_{\rho=1}^{\infty} \rho^2 e^{-(\rho-1)\delta}. \tag{46}$$

The question arises, for which values of $\delta$ this series converges, i.e., $\tilde{\zeta}(\delta) < \infty$. To derive a condition for convergence of an infinite series $\Sigma_{\rho=1}^{\infty} a_\rho$ with the single terms $a_\rho$, one can use the quotient criterion

$$\left| \frac{a_{\rho+1}}{a_\rho} \right| \leq \eta < 1 \tag{47}$$

for arbitrary values of $\rho$. Using Eq. (46), this criterion reads as

$$\frac{(\rho+1)^2 e^{-\rho\delta}}{\rho^2 e^{-(\rho-1)\delta}} \leq \eta. \tag{48}$$

Extracting the square root yields

$$\frac{(\rho+1) e^{-\rho\delta/2}}{\rho e^{-(\rho-1)\delta/2}} = \frac{(\rho+1)}{\rho e^{\delta/2}} \leq \sqrt{\eta}. \tag{49}$$

Applying the natural logarithm to this expression, one arrives at

$$-\frac{\delta}{2} + \ln\left\{ \frac{\rho+1}{\rho} \right\} \leq \ln\sqrt{\eta} = \frac{1}{2} \ln \eta. \tag{50}$$

For large values of $\rho$ the second term on the left side approaches zero. Remembering that $\eta < 1$ one obtains

$$-\frac{\delta}{2} \leq -\frac{1}{2} |\ln \eta| \tag{51}$$

and, respectively,

$$\delta \geq |\ln \eta|. \tag{52}$$

Since $\eta < 1$, this yields

$$\delta > 0 \tag{53}$$

for the decay constant. Hence for evanescent coupling, in which all orders are taken into account, the diffraction strength does not approach infinity as long as the coupling coefficients for higher-order coupling decay exponentially, while the only requirement on the decay constant $\delta$ is that $\delta > 0$.

## VI. CONCLUSIONS

In conclusion we presented an analytical expression for 2D high-order coupling in waveguide lattices, representing the Green's function of a system with general long-range waveguide interaction. The properties of the light evolution in such a system significantly change compared to a conventional system, where only adjacent waveguides experience evanescent coupling. In addition to the expected stronger broadening of the light in the lattice, the diffraction is reduced around the center of the Brillouin zone. Hence for sufficiently strong higher-order coupling, a significant fraction of the propagating light remains localized around the excited waveguide. In addition, it could be shown that in the continuum limit of the coupled mode approximation, an increase of the excitation width is not physically equivalent to a decrease in the waveguide separation. This work may help to understand advanced lattice geometries, where due to a significant higher-order coupling the conventional model of only next-neighbor interaction yields inaccurate results.

## ACKNOWLEDGMENTS

The authors wish to thank R. Iliew and F. Dreisow for fruitful discussions. A. Szameit was supported by a grant from the Jenoptik AG. We further acknowledge support by the Deutsche Forschungsgemeinschaft (Research Unit 532 "Nonlinear spatial-temporal dynamics in dissipative and discrete optical systems") and the Federal Ministry of Education and Research (Innoregio, 03ZIK051).

[1] H. Haus and L. Molter-Orr, IEEE J. Quantum Electron. **19**, 840 (1983).
[2] H. S. Eisenberg, Y. Silberberg, R. Morandotti, and J. S. Aitchison, Phys. Rev. Lett. **85**, 1863 (2000).
[3] D. Christodoulides and R. Joseph, Opt. Lett. **13**, 794 (1988).
[4] H. Eisenberg, Y. Silberberg, R. Morandotti, A. Boyd, and J. Aitchison, Phys. Rev. Lett. **81**, 3383 (1998).
[5] J. Fleischer, T. Carmon, M. Segev, N. Efremidis, and D. Christodoulides, Phys. Rev. Lett. **90**, 023902 (2003).
[6] A. Szameit, D. Bloemer, J. Burghoff, T. Schreiber, T. Pertsch, S. Nolte, A. Tunnermann, and F. Lederer, Opt. Express **13**, 10552 (2005).
[7] N. Efremidis, S. Sears, D. Christodoulides, J. Fleischer, and M. Segev, Phys. Rev. E **66**, 046602 (2002).
[8] J. Fleischer, M. Segev, N. Efremidis, and D. Christodoulides, Nature (London) **422**, 147 (2003).
[9] T. Pertsch, U. Peschel, F. Lederer, J. Burghoff, M. Will, S. Nolte, and A. Tunnermann, Opt. Lett. **29**, 468 (2004).
[10] A. Szameit, J. Burghoff, T. Pertsch, S. Nolte, A. Tunnermann, and F. Lederer, Opt. Express **14**, 6055 (2006).
[11] C. Rosberg, D. Neshev, A. Sukhorukov, W. Krolikowski, and Y. Kivshar, Opt. Lett. **32**, 397 (2007).
[12] A. Szameit, Y. Kartashov, F. Dreisow, T. Pertsch, S. Nolte, A. Tunnermann, and L. Torner, Phys. Rev. Lett. **98**, 173903 (2007).
[13] X. Wang, A. Bezryadina, Z. Chen, K. Makris, D. Christodoulides, and G. Stegeman, Phys. Rev. Lett. **98**, 123903 (2007).
[14] H. Buljan, O. Manela, R. Pezer, A. Vardi, and M. Segev, Phys. Rev. A **74**, 043610 (2006).
[15] O. Manela, M. Segev, and D. Christodoulides, Opt. Lett. **30**, 2611 (2005).
[16] A. Szameit, D. Bloemer, J. Burghoff, T. Pertsch, S. Nolte, and A. Tunnermann, Appl. Phys. B: Lasers Opt. **82**, 507 (2006).
[17] I. Garanovich, A. Szameit, A. Sukhorukov, T. Pertsch, W. Krolikowski, S. Nolte, D. Neshev, A. Tunnermann, and Y. Kivshar, Opt. Express **15**, 9737 (2007).
[18] I. Garanovich, A. Sukhorukov, and Y. Kivshar, Phys. Rev. E **74**, 066609 (2006).
[19] H. Trompeter, T. Pertsch, F. Lederer, D. Michaelis, U. Streppel, A. Braeuer, and U. Peschel, Phys. Rev. Lett. **96**, 023901 (2006).
[20] R. Gordon, Opt. Lett. **29**, 2752 (2004).
[21] R. Iwanow, D. May-Arrioja, D. Christodoulides, G. Stegeman, Y. Min, and W. Sohler, Phys. Rev. Lett. **95**, 053902 (2005).
[22] A. Szameit, F. Dreisow, H. Hartung, S. Nolte, A. Tunnermann, and F. Lederer, Appl. Phys. Lett. **90**, 241113 (2007).
[23] U. Peschel, T. Pertsch, and F. Lederer, Opt. Lett. **23**, 1701 (1998).
[24] A. Szameit, T. Pertsch, S. Nolte, A. Tunnermann, and U. Peschel, J. Opt. Soc. Am. B **24**, 2632 (2007).
[25] R. Morandotti, U. Peschel, J. S. Aitchison, H. S. Eisenberg, and Y. Silberberg, Phys. Rev. Lett. **83**, 4756 (1999).
[26] T. Pertsch, P. Dannberg, W. Elflein, A. Braeuer, and F. Lederer, Phys. Rev. Lett. **83**, 4752 (1999).
[27] H. Trompeter, W. Krolikowski, D. N. Neshev, A. S. Desyatnikov, A. A. Sukhorukov, Y. S. Kivshar, T. Pertsch, U. Peschel, and F. Lederer, Phys. Rev. Lett. **96**, 053903 (2006).
[28] A. Yariv, *Optical Electronics*, 4th ed. (Saunders College, Philadelphia, 1991).
[29] A. Szameit, T. Pertsch, F. Dreisow, S. Nolte, A. Tunnermann, U. Peschel, and F. Lederer, Phys. Rev. A **75**, 053814 (2007).
[30] A. Szameit, F. Dreisow, T. Pertsch, S. Nolte, and A. Tunnermann, Opt. Express **15**, 1579 (2007).
[31] N. Efremidis and D. Christodoulides, Phys. Rev. E **65**, 056607 (2002).
[32] A. Szameit, H. Hartung, F. Dreisow, S. Nolte, and A. Tunnermann, Appl. Phys. B: Lasers Opt. **87**, 17 (2007).
[33] N. Efremidis and K. Hizanidis, Opt. Express **13**, 10571 (2005).
[34] E. Yablonovitch, Phys. Rev. Lett. **58**, 2059 (1987).
[35] R. Meade, A. Devenyi, J. Joannopoulosa, O. Alerhand, D. Smith, and K. Kash, J. Appl. Phys. **75**, 4753 (1994).
[36] N. Moriya, Appl. Math. Model. **30**, 816 (2006).